

## Supporting Information

# Co-regulation of the copper vacancy concentration and point defects leading to the enhanced thermoelectric performance of $\text{Cu}_3\text{In}_5\text{Te}_9$ -based chalcogenides

Min Li,<sup>a,b</sup> Yong Luo,<sup>b,\*</sup> Xiaojuan Hu,<sup>c</sup> Zhongkang Han,<sup>c,\*</sup> Xianglian Liu,<sup>a</sup> Jiaolin Cui<sup>a,\*</sup>

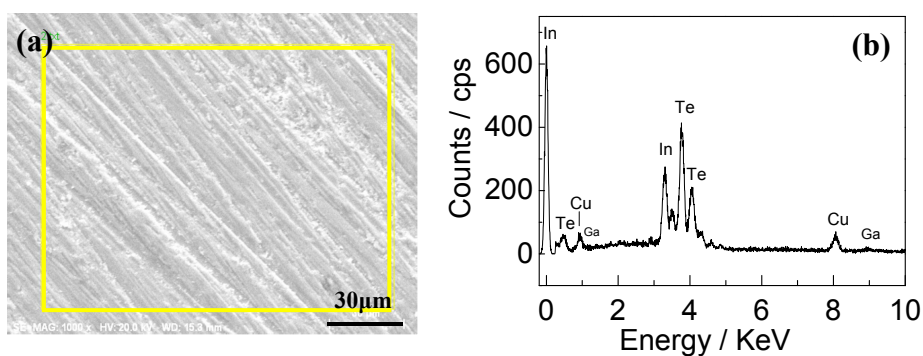


Figure S1 (a) The fracture surface of  $(\text{Cu}_{3+x}\text{In}_{5-x}\text{Ga}_x\text{Te}_9)$  ( $x=0.3$ ); (d) An EDAX pattern.

Table S1 Average molars of four elements identified in  $(\text{Cu}_{3+x}\text{In}_{5-x}\text{Ga}_x\text{Te}_9)$  ( $x=0, 0.3$ ) (taken from three different areas). The error of the compositions are about 5%.

Compounds	Cu	In	Te	Ga
$x=0$	2.86	5.08	9.04	----
$x=0.1$	2.94	5.04	9.02	0.08
$x=0.3$	3.23	4.65	9.11	0.29

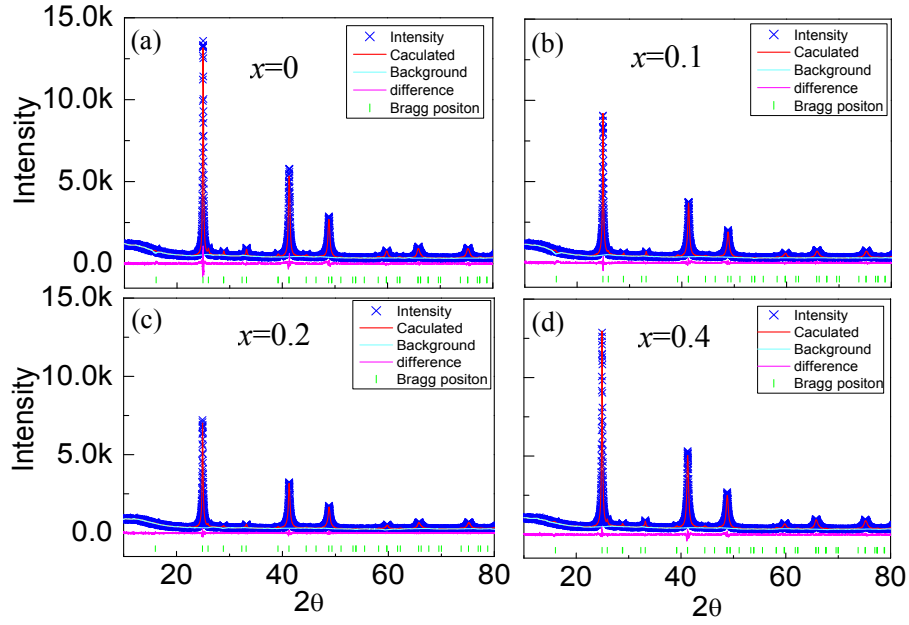


Figure S2 Rietveld refinements using the X-ray diffraction data to the samples  $\text{Cu}_{3+x}\text{In}_{5-x}\text{Ga}_x\text{Te}_9$  ( $x=0, 0.1, 0.2, 0.4$ ).

Table S2 Experimental Parameters of Powder X-ray Diffraction, and Refined Crystallographic Data of  $\text{Cu}_{3+x}\text{In}_{5-x}\text{Ga}_x\text{Te}_9$  ( $x=0$ ).

Chemical Formula	$\text{Cu}_3\text{In}_5\text{Te}_9$
Space group	P4(75)
$a$ (Å)	8.73854(7)
$b$ (Å)	8.73854(7)
$c$ (Å)	7.12986(9)
$V$ (Å <sup>3</sup> )	544.45(10)
Number of structure parameters	11
Number of profile parameters	13
$^a R_B$ (%)	4.29
$^b R_p$ (%)	4.24
$^c R_{wp}$ (%)	5.44
$^d S$	1.28

$$^a R_B = \frac{\sum |I_{O,h} - I_{C,h}|}{\sum |I_{O,h}|} \quad ^b R_p = \frac{\sum |y_i - y_{C,i}|}{\sum y_i} \quad ^c R_{wp} = \left[ \frac{\sum w_i |y_i - Y_{C,i}|^2}{\sum w_i y_i^2} \right]^{\frac{1}{2}} \quad ^d S = R_{wp} / R_{exp}$$

Table S3 Experimental Parameters of Powder X-ray Diffraction, and Refined Crystallographic Data of  $\text{Cu}_{3+x}\text{In}_{5-x}\text{Ga}_x\text{Te}_9$  ( $x=0.1$ ).

Chemical Formula	$\text{Cu}_{3.1}\text{In}_{4.9}\text{Ga}_{0.1}\text{Te}_9$
Space group	P4(75)
$a$ (Å)	8.73052(8)
$b$ (Å)	8.73052(8)
$c$ (Å)	7.10306(7)
$V$ (Å <sup>3</sup> )	541.41(5)
Number of structure parameters	12
Number of profile parameters	19
$^a R_B$ (%)	4.43
$^b R_p$ (%)	4.46
$^c R_{wp}$ (%)	5.57
$^d S$	1.25

Table S4 Experimental Parameters of Powder X-ray Diffraction, and Refined Crystallographic Data of  $\text{Cu}_{3+x}\text{In}_{5-x}\text{Ga}_x\text{Te}_9$  ( $x=0.2$ ).

Chemical Formula	$\text{Cu}_{3.2}\text{In}_{4.8}\text{Ga}_{0.2}\text{Te}_9$
Space group	P4(75)
$a$ (Å)	8.71896(5)
$b$ (Å)	8.71896(5)
$c$ (Å)	7.09668(7)
$V$ (Å <sup>3</sup> )	539.49(9)
Number of structure parameters	13
Number of profile parameters	29
$^a R_B$ (%)	4.69
$^b R_p$ (%)	4.90
$^c R_{wp}$ (%)	6.00
$^d S$	1.23

Table S5 Experimental Parameters of Powder X-ray Diffraction, and Refined Crystallographic Data of  $\text{Cu}_{3+x}\text{In}_{5-x}\text{Ga}_x\text{Te}_9$  ( $x=0.4$ ).

Chemical Formula	$\text{Cu}_{3.4}\text{In}_{4.6}\text{Ga}_{0.4}\text{Te}_9$
Space group	P4(75)
$a$ (Å)	8.690(6)
$b$ (Å)	8.690(6)
$c$ (Å)	7.05(3)
$V$ (Å <sup>3</sup> )	532.38(15)
Number of structure parameters	13
Number of profile parameters	29
$^a R_B$ (%)	4.37
$^b R_p$ (%)	4.20
$^c R_{wp}$ (%)	5.53
$^d S$	1.31

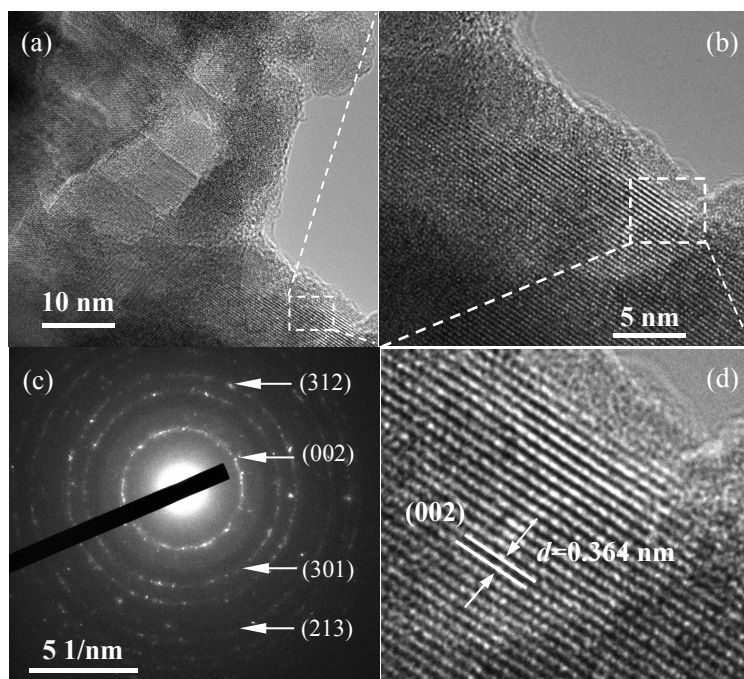


Figure S3 Microstructures of the intrinsic  $\text{Cu}_3\text{In}_5\text{Te}_9$  powder sample ( $V_c=0.11$ ,  $x=0$ ). (a) TEM image; (b) Zoomed view in (a); (c) Corresponding selected area electron diffraction (SAED) pattern; (d) Magnified image of (b).

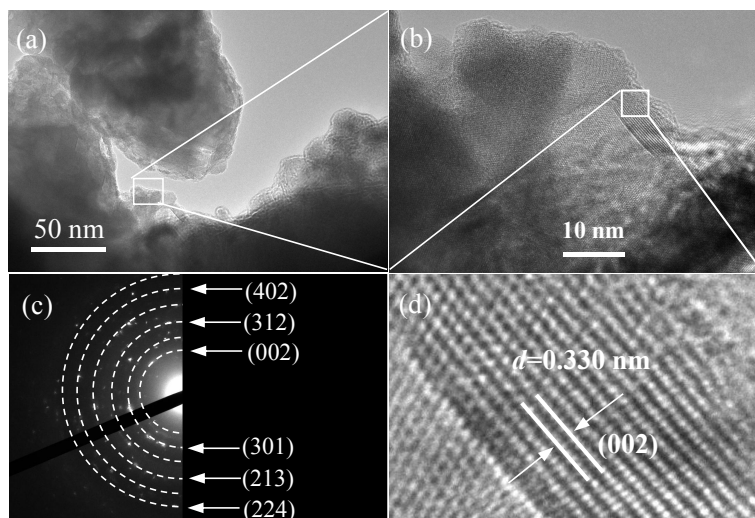


Figure S4 Microstructures of the  $\text{Cu}_{3+x}\text{In}_{5+x}\text{Ga}_x\text{Te}_9$  powder sample ( $V_c=0.078$ ,  $x=0.3$ ). (a) TEM image; (b) Zoomed view in (a); (c) Corresponding selected area electron diffraction (SAED) pattern; (d) Magnified image of (b).

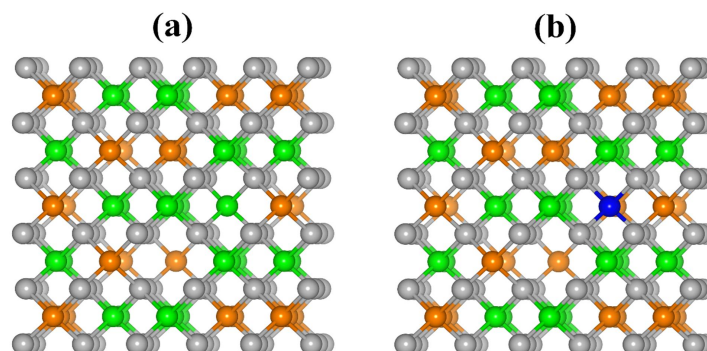


Figure S5 Crystal structures of (a)  $\text{Cu}_{10}\text{In}_{17}\text{Te}_{32}$  and (b)  $\text{Cu}_{11}\text{In}_{16}\text{GaTe}_{32}$ . Cu, In, Te, and Ga are in yellow, green, grey, and blue, respectively.

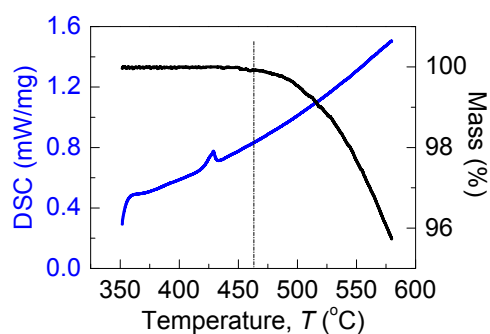


Figure S6 TGA/DSC data for  $\text{Cu}_3\text{In}_5\text{Te}_9$ , with exothermic effect at  $\sim 427$  °C, at which an order-disorder transition might occur.